# Kirin: A Quadruped Robot with High Payload Carrying Capability

Yueheng Zhou[1], Ming Liu[3], Chaoyang Song[1], Jianwen Luo[2*]

***Abstract*— The quadruped robot is a versatile mobile platform with potential ability for high payload carrying. However, most of the existing quadruped robots aim at high maneuverability, highly dynamic and agile locomotion. In spite of this, payload carrying is still an indispensable ability for the quadruped robots. Design of a quadruped robot with high payload capacity is yet deeply explored. In this study, a 50 kg electrically-actuated quadruped robot, Kirin, is presented to leverage the payload carrying capability. Kirin is an characterized with prismatic quasi-direct-drive (QDD) leg. This mechanism greatly augments the payload carrying capability. This study presents several design principles for the payload-carrying-oriented quadruped robots, including the mechanical design, actuator parameters selection, and locomotion control method. The theoretical analysis implies that the lifting task tends to be a bottleneck for the existing robots with the articulated knee joints. By using prismatic QDD leg, the payload carrying capability of Kirin is enhanced greatly. To demonstrate Kirin's payload carrying capability, in preliminary experiment, up to 125 kg payload lifting in static stance and 50 kg payload carrying in dynamic trotting are tested. Whole body compliance with payload carrying is also demonstrated.**

## I. Introduction

The development of various biomimetic quadruped robots is inspired by the graceful and agile legged locomotion of animals [1]. Biomimetic robots are extensively used as scientific tools to investigate and justify the hypotheses in biomechanics and neuroscience fields [2], [3]. Legged locomotion also boosts the practice in payload carrying transportation on unstructured terrains [1], [4]–[6]. The payload carrying task requires the quadruped robots to function as a versatile mobile platform over rough terrains, which can be deemed as a complement to wheeled vehicles. Currently, with the maturity of the technology and theory in legged locomotion field, quadruped robots becomes one of the well-known biomimetic robots deployed in the real-world applications [7]–[9]. In the foreseeable future, Quadruped robots will be able to carry goods and execute long-duration outdoor operations without human intervene. During the last decades, a series of milestone quadruped robots were reported, some of which are capable of high speed running, jumping or backward flipping [7], [10]. However, the payload capacity, one of the most critical metrics for mobile platform, has yet been fully explored.

*This work was supported in part by National Natural Science Foundation of China under Grant 51905251. *(Corresponding author: Jianwen Luo. Email: luojianwen1123@gmail.com)*

[1]Y. Zhou and C. Song is with the Southern University of Science and Technology (SUSTech), Shenzhen, 518055, China. *songcy@sustech.edu.cn*

[2]J. Luo is with Hong Kong University of Science and Technology (Guangzhou), Guangzhou, 510000, China.

[3]M. Liu is with Hong Kong University of Science and Technology, Hong Kong, China.


Fig. 1. The electrically actuated quadruped robot, Kirin, for high payload carrying. The self-weight of Kirin is 50 kg and is capable of lifting up to 125 kg payload in the static standing state. Kirin has 12 DoF's with two articulated joints and one prismatic joint for each leg. The dimension of the robot is 700 $\times$ 240 $\times$ 600 mm. The robot is untethered, with battery, electric boards, motor drivers and sensors embedded in the main body.

To increase the payload carrying capacity, many strategies are proposed based on the actuators and evaluation criteria. Some of the early quadruped robots adopted hydraulic actuators due to the high power-to-weight ratio. However, the bulky auxiliary devices in hydraulic system result in the large self-weight of the robot [11], [12]. Therefore, the payload to weight ratio (payload capacity, PLC) and energy efficiency of hydraulic quadruped robots are relatively low. The criterion for energy efficiency, cost of transport (CoT), of Boston Dynamics hydraulic BigDog is 15, which is significantly higher than those of humans or animals of similar scale [7]. Electrically-actuated quadruped robots are developed to make up these shortcomings. By integrating electric motors with the passive dynamics and elastic elements, energy is stored by kinetic or elastic components [13]–[16], and quadruped robot efficiency is improved [17]. CoT ($P/mgv$) metric draws more interests in the high-speed dynamic locomotion, such as jumping, running, back-flipping, etc [10], while the external payload is not taken into account.

As for the payload capacity (PLC), the existing quadruped robots is usually lower than 1:1 under normal walking speed according to the available reports. For example, walking test on a commercially 12 kg quadruped robot Unitree A1 shows that 10 kg payload is achievable with a speed of 0.1 m/s [18]. 30 kg SpotMini is able to carry 14 kg payload. 50 kg ANYmal can carry 10 kg payload [19]. Baby elephant, electrical-hydraulically actuated with parallel legs, has payload of 100 kg with the PLC of 0.77 [20]. PLC of some representative quadruped robots under 150 kg are listed in Fig. 2. It is believed that the essential improvement of payload capacity is waiting to be explored.

In this study, some design principles are proposed to

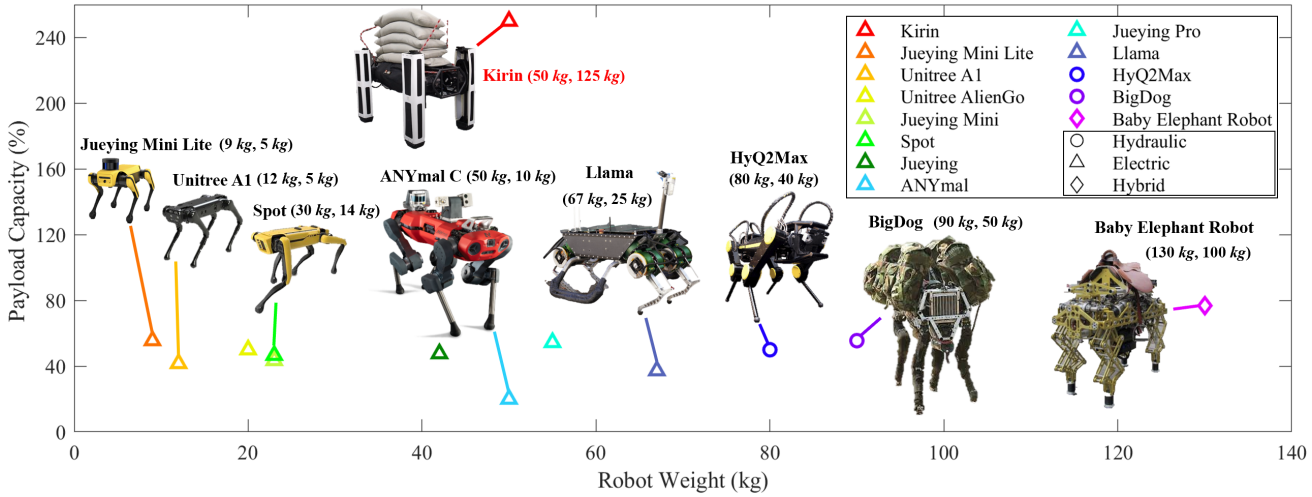


Fig. 2. The overview of PLC, which is the ratio of payload to weight. The reported quadruped robots with varied self-weight below 140 $rmkg$ are listed based on the available information. The first and second value with each robot are the self-weight and the payload weight respectively. At the current stage, the experiment result for Kirin's maximum payload is 125 kg. Therefore, PLC of Kirin is 250 %. Hydraulic, electric and hybrid actuators are labelled as circle, triangle and diamond respectively. Among the quadruped robots above, HyQ2Max and Big Dog are hydraulically. The quadruped robots below 80 kg are all electrically actuated.

improve the payload carrying capability towards the practical demand. A novel quadruped robot, Kirin, was developed, aiming at the effective high payload carrying capability (Fig.1(b)). The mechanism of Kirin robot is designed different from current typical configuration. A trade-off has been made between the payload capacity and locomotion through optimization within the strength limitation of mechanical parts and advances in actuator technology. The design principles are also discussed for achieving a transportation-oriented quadruped robot. This study aims to propose some design principles to push the payload limits higher, and promote the carrying ability towards the demands of practical applications. The contributions of this study mainly lie in the following two fold:

1) A quadruped robot, Kirin, is developed, aiming at the dynamic locomotion with high payload capability. The novel prismatic QDD leg is introduced.

2) The design principles are discussed for achieving a transportation-oriented quadrupedal robot by analyzing the payload carrying demand. A trade-off has been made between the payload capacity and locomotion through optimization within the strength limitation of mechanical parts and advances in actuator technology.

The rest of the article is organized as follows. Section II introduces the design principles of Kirin quadruped robot for payload carrying, and describes how the design principles are implemented on Kirin. Section III shows the verification of Kirin's payload capacity, and the accomplishment of tasks such as lifting, trotting with payload carrying. This line of research is discussed and concluded in Section IV.

## II. Design Principles for Payload Carrying

In this study, several principles are claimed for designing payload-carrying-oriented quadruped robots. Among the most critical issues based on the previous robot design, several are listed below:

1) The robot should have high payload capacity to carry considerable weights. Considering that the potential application of legged robot is challenging in unstructured terrains and disaster rescue scenarios, the robot need to bear manipulator arm, sensing devices, etc [21], [22]. Correspondingly, reliable and robust mechanical design are required.

2) The robot should have reliable weight lifting performance for loading/unloading. Loading/unloading process is an essential factor in transportation. Lifting involves intensive positive work against gravity, which might be the bottleneck of the biomimetic quadruped robots.

3) The improvement of payload carrying capability should not sacrifice the agility of legged locomotion, including the adaptability to rough terrains [4] and locomotion velocities [14], self-righting capability [23], etc.

### A. Mechanism Design for High Payload Capacity

A high-payload-capacity robot usually needs high-torque actuators [24]. For legged robots, three mainstream strategies have been developed including high-ratio geared motor with torque sensors, high-ratio geared motor with series elastic actuators, and low-ratio geared quasi-direct-drive (QDD). Considering that different types of electromagnetic motors are available off-the-shelf, the gear transmission is thus a critical customized component to regulate the power output. A 2 kg customized QDD with 16:1 planetary gear is selected to drive Kirin's joints. The rated power is 0.4 kW, and rated torque is 40 Nm while the peak power is 1 kW, and the peak torque can reach up to 200 Nm. Thanks to high torque density of electric actuators, the low gear reduction also demonstrated the feasibility for high payload capacity.

QDD is appealing for its compatibility with legged locomotion dynamic [10], [25], [26]. Legged locomotion consists of repeating periodic events involving impact, high-force interaction with uncertain terrains, and rapid leg swing

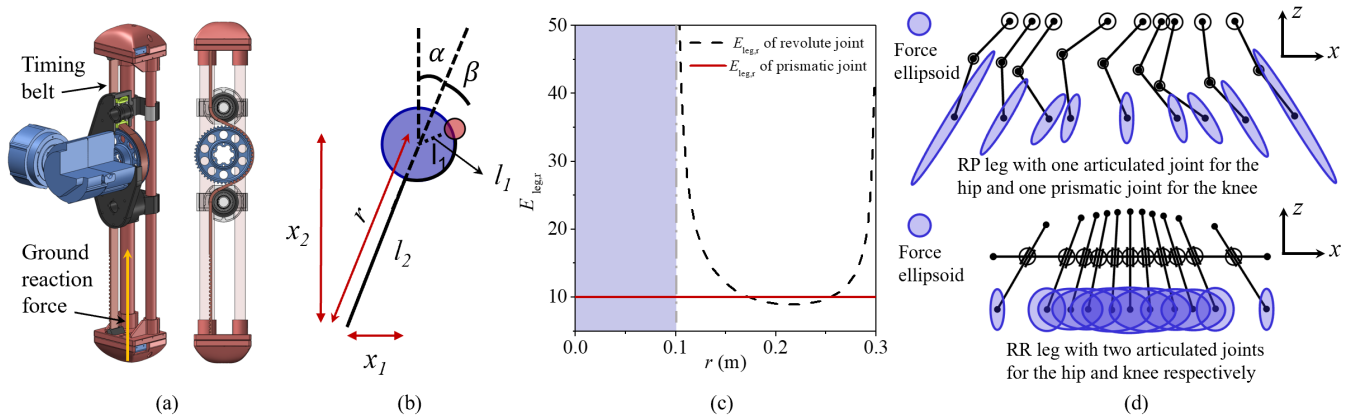


Fig. 3. (a) Assembly of the actuators and mechanical components in prismatic leg. And force analysis of main component including supporting sliders, pulley, and belt. The robot torso suspends by the belt and can move up and down on the supporting sliders. (b) Infinitesimal kinematics analysis of our prismatic leg. The $E_{leg,r}$ curve with varied height r shows the constant torque output feature (c). (d). The force ellipsoid of articulated leg (upper) and prismatic leg in Sagittal plane ($x-z$ plane), showing the reliable supporting forces of prismatic leg during different configuration.

[27]. Actuators must be mechanically robust to these impacts. High gear reduction induces high gear friction, and absorbs the peak torque directly [10]. The reduction gears are easily fatigued and damaged irreversibly. For QDD, due to the low actuator inertia and low gear friction, impact force is backdrivable to the actuators, and can be handled by compliance control [28]. Besides, the proprioception of QDD avoids using additional torque or force sensors to implement force control, contact detection and dynamic identification functionalities on robots.

As for the mechanical structure, legs should be mechanically robust and light-weight. Light-weight design helps decrease the leg's inertia and improve the kinematic performance and terrain adaptability. Prismatic structure is adopted for Kirin due to the straightforward and lightest structure compared with the leg of revolute joints [7]. The leg consists of two stainless steel tubular sliders of 2 $\mathrm{mm}$ thickness and one timing belt of 30 $\mathrm{mm}$ width for body suspension. As shown in Fig. 3(a), the sliders are aligned in the sagittal plane, where the mechanical leg is most stressed. The diameter of proximal sliders (30 $\mathrm{mm}$) is thicker than that of the distal (22 $\mathrm{mm}$) to overcome the longitudinal load on the tube surface and the cross section. The foot-end are wrapped with soft silicon foot pad made of Ecoflex00-30 for impact mitigation.

The illustrated analysis of the leg stress is shown in Fig. 3(a). The total torso and actuators weight are concentrated on the body. Four legs of 9.68 $\mathrm{kg}$ accounts for 7 $\%$ of the total weight. The sliders can supply over 4.6 $\mathrm{kN}$ compression force against ground reaction force theoretically. The body and payload are supported by the timing belt. The timing belt is fixed on the top of the slider and bear the tension force. The tensile strength of belt is 9 $\mathrm{kN}$ with a 4 $\%$ elongation. When the body moves up and down, the power is transmitted by the pulley. Every gear tooth of belt have a shear strength over 60 $\mathrm{N/mm^2}$, and the max transmission force reach 9.6 $\mathrm{kN}$. The mating tooth number should be as low as possible to reduce the frictions. Thus, every component of the leg is optimized to have the same ultimate stress to guarantee the mechanical reliability for the legged locomotion.

### *B. Force Ellipsoid Analysis for Payload Lifting*

Payload lifting during transportation is a crucial task. Legs are equivalent to an independent suspension, and have the advantages over wheeled vehicles in terms of the flexible adjustment of body in both horizontal and vertical directions. Quadruped robots can execute some tasks at a certain height, and the free lifting enables the payload loading/unloading on the robot torso in the transportation process. Lifting poses two requirements for the robot configuration design:

1) Lifting should not limit payload capacity during transportation.

2) The payload capacity and locomotion should not be discounted due to the torso height variation.

Infinitesimal kinematics is used to analyze the energy-mechanical conversion in radial direction during the lifting process [29]. The pulley-belt structure is illustrated in Fig. 3(a). The individual motor angles of hip flexion/extension (HFE) and leg elongation/contraction (LEC) joints $q := (\theta_1, \theta_2)^T$ expressed in the world frame are mapped to difference and mean coordinates according to:

$$a := [\alpha, \beta]^T = [0, \pi]^T + \begin{bmatrix} 1 & 0 \\ 0 & 1 \end{bmatrix} q. \tag{1}$$

it is convenient to analyze in polar coordinates:

$$P := [\alpha, r]^T := [\alpha, l_2 - (\pi - \beta) l_1]^T, \tag{2}$$

as well as the Cartesian coordinates:

$$X = [x_1, x_2]^T = [(r + l_2) sin\alpha, (r + l_2) cos\alpha]^T. \tag{3}$$

Because only vertical kinematics is concerned, the radial coordinate (r) and the radial infinitesimal kinematics of the leg are invariant for our leg configuration:

$$E_{leg,r}(r) = \frac{\partial \beta}{\partial r} = \frac{1}{l_1}. \tag{4}$$

For the conventional two-segment legs with articulated joints [29]:

$$E_{leg,r}(r) = \frac{\partial \beta}{\partial r} = \frac{r^2 - l_1^2 + l_2^2}{r^2 l_1 \sqrt{-\frac{l_1^4 + \left(l_2^2 - r^2\right)^2 - 2l_1^2(l_2^2 + r^2)}{l_1^2 r^2}}}. \quad (5)$$

when composed with the gear ratio $E_m$, the infinitesimal map from motor shaft torque to radial toe force is: $E_{tot,r}(r) = \frac{\partial q}{\partial \beta}\frac{\partial \beta}{\partial r} = E_m E_{leg,r}(r)$. To enable the high payload, the leg configuration should allow the motor to provide higher torque. If the robot stands vertically without lateral external force, the force direction of support leg is radial. The Jacobian matrix is equal to the $(1/E_{leg,r}(r))$ in this way. Assuming that the max torque limit for the motor is constant value of F. The maximal ground reaction force is $\tau = F/E_{leg,r}(r)$. To facilitate the comparison, we use the same parameters $l_1$ = 0.1 m , $l_2$ = 0.2 m here. As shown in Fig. 3(c), $E_{leg,r}(r)$ curves varied with height $(r)$ for revolute while $E_{leg,r}(r)$ is invariance of $1/l_1$ for our prismatic configurations. Only in the narrow range from 0.17 m to 0.253 m with maximal difference of 1.09 that the revolute joints showed advantages. There exist an asymptote of 0.1 m when the $E_{leg,r}(r)$ towards positive infinity. This indicates that the prismatic joints output constant torque in the vertical lifting process.

Force ellipsoid is utilized for analyzing the contact force mapped from the joint torques. Given that the joint torque $\tau$ satisfies $\tau^T\tau = 1$, which is a unit sphere in the joint torque space. Considering $\tau = J^T F$, the contact force ellipsoid is formulated as $F^T A F = 1$, where $A = JJ^T$ defines the contact force ellipsoid. The eigenvectors and the square roots of eigenvalues of $A$ that define the shape of the force ellipsoid. The Jacobian of Kirin's prismatic leg is:

$$J = \begin{bmatrix} 0, & -c_\phi l_\omega, & -s_\phi \\ -c_\theta c_\phi l_\omega - s_\theta l_1, & s_\theta s_\phi l_\omega, & -s_\theta c_\phi \\ -s_\theta c_\phi l_\omega - c_\theta l_1, & c_\theta s_\phi l_\omega, & -c_\theta c_\phi \end{bmatrix}, \quad (6)$$

where $c_{(\cdot)} := \cos(\cdot)$ and $s_{(\cdot)} := \sin(\cdot)$. $l_\omega = l_3 + \omega$. $l_3$ is the shank length. $\omega$ denotes the angle of flexion/extension (KFE) joint (equals to 0 in this study). $l_1$ is the distance from HFE to hip adduction/abduction (HAA) joint, and $l_3$ is the distance from foot to (KFE) joint. The corresponding force ellipsoids of Kirin's prismatic leg and typical articulated leg are shown in Fig. 3(d). Prismatic leg has the inherent property that the foot could provide constant supporting forces in the vertical direction, which the articulated leg cannot. Although prismatic joint is not the type of bionic mammal joint, it is believed this feature benefits the payload carrying in transportation task.

### C. Locomotion Control for Kirin

The increase in payload capacity should not be at the expense of agile locomotion, which is the advantage of legged robots over wheeled vehicle [30]. The sizes of joints and links should be carefully designed to enable the altitude adjustment and the joints should be enabled to react timely towards disturbances. Besides, control algorithm should be implemented to adapt uneven terrains. Each leg of Kirin has 3 DoFs, including HAA, HFE and LEC joints. The joint actuators are all mounted on the main body to reduce the leg inertia.

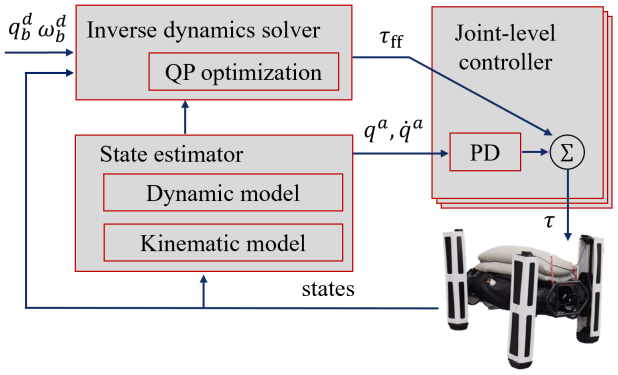


Fig. 4. Control scheme of Kirin for dynamic locomotion. The states from the sensors of Kirin is sent to state estimator as feedback. Desired joint position and velocity are sent to joint-level control for PD control. Inverse dynamics solver based on QP optimization computes the feedforward joint torques.

A force-based locomotion controller is implemented on Kirin [31]. The locomotion controller is used to track the desired motion of the main body and optimally distribute the ground reaction forces [32]. The desired forces $F_b$ and moment $T_b$ are given as:

$$\begin{cases} F_b = K_p^f(r_b^d - r_b^a) + K_i^f \int (r_b^d - r_b^a) + \\ \qquad K_d^f(v_b^d - v_b^a) + m\ddot{r}_b^d + \sum m_i g \\ T_b = K_p^t \log\left(q_b^d \cdot (q_b^a)^{-1}\right) + K_i^t \int \log\left(q_b^d \cdot (q_b^a)^{-1}\right) \\ \qquad + K_d^t \log\left(\omega_b^d \cdot (\omega_b^a)^{-1}\right) + \sum r_i \times m_i g \end{cases}, \quad (7)$$

where $r_b^d$, $v_b^d$, $\ddot{r}_b$, $q_b^d$, $\omega_b^d$ represent the desired position, linear velocity, linear acceleration, rotation matrix and angular velocity of the robot torso. $r_b^a$, $v_b^a$, $q_b^a$ and $\omega_b^a$ represent the actual position, linear acceleration, rotation matrix and angular velocity of the robot torso.

The desired contact force $F_c$ is computed by inverse dynamics solver based on quadratic programming (QP) optimization. Joint torques $\tau$ is computed using $\tau = J^T F_c$ . The joint position and velocity are sent to joint-level controller as PD feedback control. The QP formulation is given as:

$$F_c = \arg\min_F (AF - B)^T Q (AF - B) + F^T R F$$
$$s.t. \begin{cases} \tau_{min} \le J^T F \le \tau_{max} \\ -\mu F_{iz} \le F_{ix} \le \mu F_{iz} \\ -\mu F_{iz} \le F_{iy} \le \mu F_{iz} \\ H_i F_i = 0 \end{cases}, \quad (8)$$

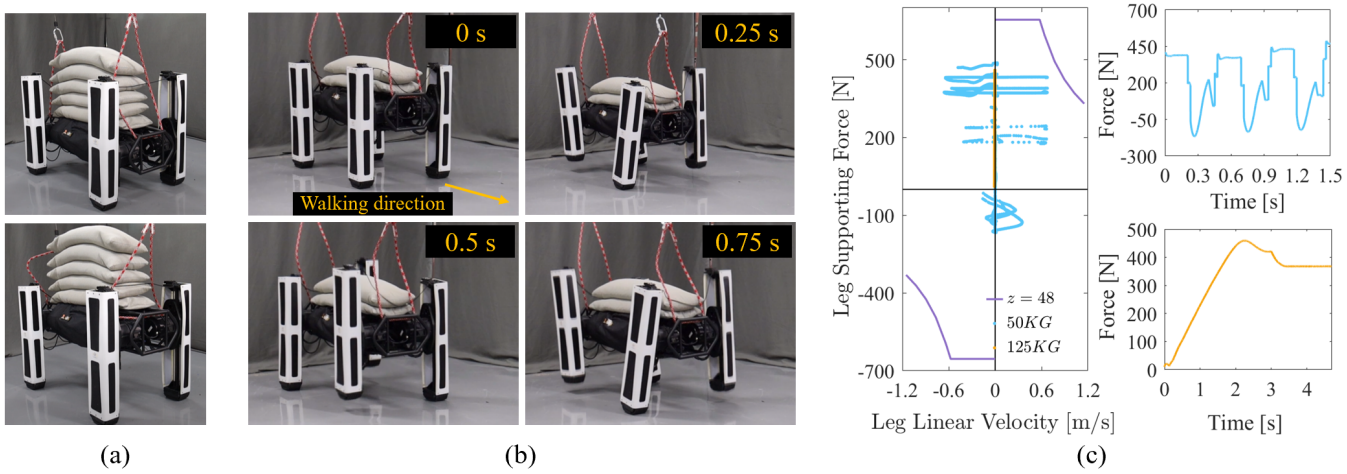


Fig. 5. (a) Kirin could easily lift 125 $kg$ (5 sandbags, each of which weighs 25 kg) payload from initial lying down state to standing state. (b) Screenshots of Kirin trotting with payload of 50 kg. The gait cycle is 0.5 s. (c) The forces curves of LEC joint during lifting with 125 kg payload, and walking with 50 kg payload. Kirin still work within the rated region of motor.

TABLE I
SPECIFICATIONS OF QUADRUPED ROBOT KIRIN

| Property | Parameters |
|---|---|
| Dimensions (L×W×H) ($mm$) | 700 × 240 × 600 |
| Total weight ($kg$) | 50 |
| Active DoF number | 12 |
| Motion range of hip roll joint (°) | 280 |
| Motion range of hip pitch (°) | 360 |
| Motion range of knee joint ($mm$) | 300 |
| Electric actuator | Customized QDD |
| Force sensing | None |
| Inertial measurement unit (IMU) | XSense MTI-G-710 |
| Computing board | Nvidia Jetson TX2 |
| Joint peak torque (Nm) | 150 |
| Joint peak speed (rpm) | 130 |
| Motor driver | G-SOLWH120/100EES |

* Due to the safety consideration, 125 kg is the experiment result at the current stage. More payload is to be tested.

where $F_{ix}, F_{iy}$, and $F_{iz}$ are the components of $F_i$. $\tau_{min}$ and $\tau_{max}$ are the joint torque limits. $H_i$ is the selection matrix for the contact feet. $\mu$ is the coefficient of friction. $F_c \in \Re^{3N\times 1}$ is the concatenated vector of the contact forces. $N$ is the number of contact feet. The diagonal matrix $Q$ and $R$ are the weight matrix. $A$ and $B$ are given as:

$$A = \begin{bmatrix} \cdots & I & \cdots \\ \cdots & \hat{r_{ci}} & \cdots \end{bmatrix}, \quad B = \begin{bmatrix} F_b \\ T_b \end{bmatrix}. \tag{9}$$

## III. EXPERIMENT

In this section, preliminary experiments are conducted to validate the payload carrying performance of Kirin. The specifications of Kirin is listed in Table. I. The electrical subsystem of the robot includes modular embedded computer, battery, motor driver and sensors. Nvidia TX2 is deployed in the main body of Kirin as the controller. RT-Linux is installed with real-time patch on TX2. Elmo drivers are used to run the motor servo loop and connected through EtherCAT. In the next subsections, experiment results are demonstrated.

### A. Payload Lifting and Walking Test

This subsection presents the preliminary results of payload lifting and walking tests. Sandbags, each of which weighs 25 kg, were used as payload. Static payload lifting test was conducted first, and Kirin could stand up with 175 kg payload on the torso. 125 kg is the maximum payload of Kirin for lifting test. Kirin was initially set to lower the torso to lie down. Five sandbags were loaded on the back of Kirin and the payload is lift up as shown in Fig. 5(a). Pre-computed control torques were applied to drive the body to reach the desired height from 0.3 m to 0.65 m with four legs supporting on the ground. Usually, the torque of the KFE joint would suffer two times that of the articulated leg [23]. Benefiting from the prismatic LEC joint of Kirin, the torque of torso remained constant during lifting and is similar to that of the HAA/HFE joint. LEC joint data was recorded during lifting as shown in Fig. 5(c). The yellow lines are the joint force of one leg. The static forces during lifting up is near 400 N, which was equivalent to 174 kg total weight, ie., self-weight (50 kg) plus the payload (125 kg). This value was calculated from the feedback of motor current, implying the good proprioception of the QDD actuator. At the initial phase of lifting, a peak force is 457 N due to the acceleration process. The force-linear sliding velocity diagram of LEC joint is plotted in left of Fig. 5(c). The purple lines are the rated motor power, which was the bounds of the available working region of Kirin. The lifting velocity was 0.056 m/s, and the max forces are below the the bounds of rated operating range of motor. Considering the rated motor

power, a safety factor of about 0.65 was taken.

The payload capacity is also tested in the walking task to evaluate Kirin's payload performance (Supplementary Video S1). As shown in Fig. 5(b), Kirin is trotting at a gait cycle of 0.5 $\mathrm{s}$ with 50 $\mathrm{kg}$ payload, which is equal to the robot's own weight. The max trotting speed of Kirin in Gazebo simulation is up to 1.2 $\mathrm{m/s}$. The speed of the walking test experiment is set to 0.3 $\mathrm{m/s}$. With the 50 $\mathrm{kg}$ payload, the locomotion speed is not discounted. The peak forces in the supporting phase is around 500 $\mathrm{N}$, corresponding to 30.5 $\mathrm{Nm}$ of the motor, which was within the bounds purple lines. The symmetric trotting gait guarantees two-foot to be kept supporting on the ground. Although 50 $\mathrm{kg}$ payload in walking test is around the half of 125 $\mathrm{kg}$ payload in lifting test, it is not always applicable for articulated joints, where the maximum payload capacity might occur in the lifting process. It is believed that the payload capacity in walking test can be further evaluated by fully exploiting the capacity of the motors.

### *B. Posture Adjustment Test*

This subsection presents the posture adjustment test to demonstrate the whole-body compliance. Due to the wide motion range of each joint, Kirin's flexibility enables it to easily reach a wide range of orientations without moving its feet. The motion range of HAA, HFE, and LEC are 280°, 360°, and 0.3 $\mathrm{m}$, respectively. Considering the mechanical interference, the pitch angle, yaw, and roll angles could reach 25°, 30°, and 90° as shown in Fig. 6(a). The flexible torso is potentially helpful when passing through narrow passages or self-righting after falling. In the experiment, two wood plates are placed under the front feet of Kirin and lifted up to generate disturbance to test the joint compliance as shown in Fig. 6(b). The posture of Kirin is measured through IMU as feedback to keep the main body horizontal. The torso altitudes, LEC joint positions, and forces are visualized in Fig. 6(c). Pitch angle of Kirin torso has the fluctuated angle magnitude of 2.5° while other position errors are negligible, demonstrating the effectiveness of joint torque control of Kirin.

## IV. Discussions and Conclusions

This study presents a novel quadruped robot, Kirin. The payload carrying capability is analyzed. Three major design principles are summarized and implemented on Kirin. The principles include QDD motors, prismatic leg designs for payload lifting properties, and dynamics locomotion performances. Kirin is capable of static supporting payload of 175 $\mathrm{kg}$ (including the self-weight of the robot), a lifting payload of 125 $\mathrm{kg}$, and a trotting with payload of 50 $\mathrm{kg}$ from the experimental verification of LEC joint torque and velocity. Given the self-weight of 50 $\mathrm{kg}$, Kirin outperforms the payload capacity of animals and existing published quadruped robots of similar body size. Kirin is featured with the prismatic actuated leg that can provide linear torques in lifting task, and the supporting force is independent of body-height. Lifting and walking tests are decomposed from transportation application, because it is found that lifting is

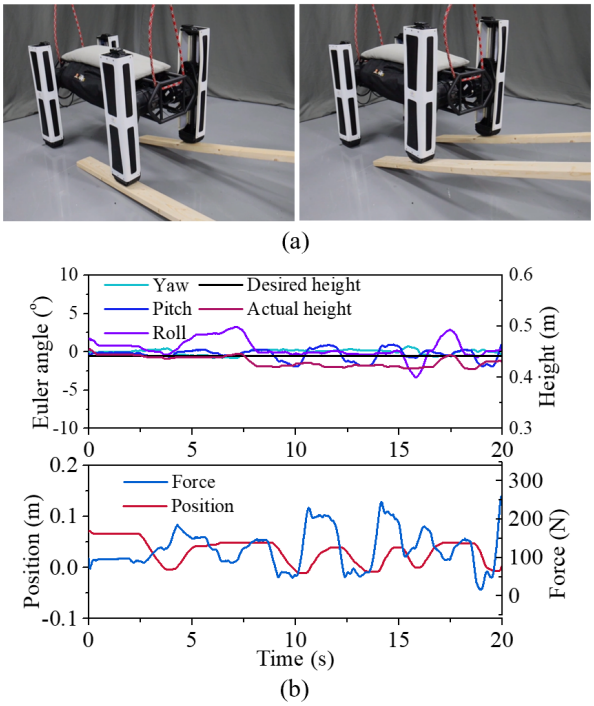


Fig. 6. (a) Joint compliance test of Kirin to simulate the foot placement on uneven terrains. (b) The record attitude of torso and LEC joint when Kirin adaptive to the random disturbance using the wood plates.

of equally important for payload carrying. Sometimes lifting turns out to be the bottleneck for some robots with articulated knee joints, as theoretically analyzed by kinematics and force ellipsoid comparison. Kirin's prismatic joint is simply composed of an electromagnetic motor, pulley and timing belt, which can effectively convert rotation to sliding at low friction. The legs can also be designed as a drop-in replacement when they are implemented on the Kirin robot. Future work will include unknown payload identification and adaptive control so that Kirin could handle online payload variation.

## APPENDIX

A supplementary video of experiment is available.

## References


[1] A. J. Ijspeert, "Biorobotics: Using robots to emulate and investigate agile locomotion," *Science*, vol. 346, no. 6206, pp. 196–203, 2014.

[2] A. Spröwitz, A. Tuleu, M. Vespignani, M. Ajallooeian, E. Badri, and A. J. Ijspeert, "Towards dynamic trot gait locomotion: Design, control, and experiments with cheetah-cub, a compliant quadruped robot," *The International Journal of Robotics Research*, vol. 32, no. 8, pp. 932–950, 2013.

[3] D. Kim, S. J. Jorgensen, J. Lee, J. Ahn, J. Luo, and L. Sentis, "Dynamic locomotion for passive-ankle biped robots and humanoids using whole-body locomotion control," *The International Journal of Robotics Research*, vol. 39, no. 8, pp. 936–956, 2020.

[4] J. Lee, J. Hwangbo, L. Wellhausen, V. Koltun, and M. Hutter, "Learning quadrupedal locomotion over challenging terrain," *Science Robotics*, vol. 5, no. 47, p. eabc5986, 2020.

[5] H. Zhu, D. Wang, N. Boyd, Z. Zhou, L. Ruan, A. Zhang, N. Ding, Y. Zhao, and J. Luo, "Terrain-perception-free quadrupedal spinning locomotion on versatile terrains: Modeling, analysis, and experimental validation," *Frontiers in Robotics and AI*, vol. 8, 2021. [Online]. Available: https://www.frontiersin.org/article/10.3389/frobt.2021.724138

[6] J. Luo, Y. Su, L. Ruan, Y. Zhao, D. Kim, L. Sentis, and C. Fu, "Robust bipedal locomotion based on a hierarchical control structure," *Robotica*, vol. 37, no. 10, pp. 1750–1767, 2019.

[7] Y. Zhong, R. Wang, H. Feng, and Y. Chen, "Analysis and research of quadruped robot's legs: a comprehensive review," *International Journal of Advanced Robotic Systems*, vol. 16, no. 3, p. 1729881419844148, 2019.

[8] X. Meng, S. Wang, Z. Cao, and L. Zhang, "A review of quadruped robots and environment perception," in *2016 35th Chinese Control Conference (CCC)*, 2016, pp. 6350–6356.

[9] C. Gehring, "Planning and control for agile quadruped robots," Ph.D. dissertation, ETH Zurich, 2017.

[10] B. Katz, J. D. Carlo, and S. Kim, "Mini cheetah: A platform for pushing the limits of dynamic quadruped control," in *2019 International Conference on Robotics and Automation (ICRA)*, 2019, pp. 6295–6301.

[11] J.-W. Chung, I.-W. Park, and J.-H. Oh, "On the design and development of a quadruped robot platform," *Advanced Robotics*, vol. 24, no. 1-2, pp. 277–298, 2010.

[12] J. Luo, Y. Fu, and S. Wang, "3d stable biped walking control and implementation on real robot," *Advanced Robotics*, vol. 31, no. 12, pp. 634–649, 2017.

[13] P. A. Bhounsule, J. Cortell, and A. Ruina, "Design and control of ranger: an energy-efficient, dynamic walking robot," in *Adaptive Mobile Robotics*. World Scientific, 2012, pp. 441–448.

[14] M. Hutter, C. Gehring, M. A. Höpflinger, M. Blösch, and R. Siegwart, "Toward combining speed, efficiency, versatility, and robustness in an autonomous quadruped," *IEEE Transactions on Robotics*, vol. 30, no. 6, pp. 1427–1440, 2014.

[15] J. W. Hurst, J. E. Chestnutt, and A. A. Rizzi, "The actuator with mechanically adjustable series compliance," *IEEE Transactions on Robotics*, vol. 26, no. 4, pp. 597–606, 2010.

[16] J. Luo, S. Wang, Y. Zhao, and Y. Fu, "Variable stiffness control of series elastic actuated biped locomotion," *Intelligent Service Robotics*, vol. 11, no. 3, pp. 225–235, 2018.

[17] S. Seok, A. Wang, M. Y. Chuah, D. J. Hyun, J. Lee, D. M. Otten, J. H. Lang, and S. Kim, "Design principles for energy-efficient legged locomotion and implementation on the mit cheetah robot," *Ieee/asme transactions on mechatronics*, vol. 20, no. 3, pp. 1117–1129, 2014.

[18] Y. Sun, W. Ubellacker, W. Ma, X. Zhang, C. Wang, N. Csomay-Shanklin, M. Tomizuka, K. Sreenath, and A. Ames, "Online learning of unknown dynamics for model-based controllers in legged locomotion," *IEEE Robotics and Automation Letters*, 2021.

[19] M. Hutter, C. Gehring, D. Jud, A. Lauber, C. D. Bellicoso, V. Tsounis, J. Hwangbo, K. Bodie, P. Fankhauser, M. Bloesch, R. Diethelm, S. Bachmann, A. Melzer, and M. Hoepflinger, "Anymal - a highly mobile and dynamic quadrupedal robot," in *2016 IEEE/RSJ International Conference on Intelligent Robots and Systems (IROS)*, 2016, pp. 38–44.

[20] F. Gao, C. Qi, Q. Sun, X. Chen, and X. Tian, "A quadruped robot with parallel mechanism legs," in *2014 IEEE International Conference on Robotics and Automation (ICRA)*, 2014, pp. 2566–2566.

[21] G. Tournois, M. Focchi, A. Del Prete, R. Orsolino, D. G. Caldwell, and C. Semini, "Online payload identification for quadruped robots," in *2017 IEEE/RSJ International Conference on Intelligent Robots and Systems (IROS)*. IEEE, 2017, pp. 4889–4896.

[22] F. Jenelten, T. Miki, A. E. Vijayan, M. Bjelonic, and M. Hutter, "Perceptive locomotion in rough terrain – online foothold optimization," *IEEE Robotics and Automation Letters*, vol. 5, no. 4, pp. 5370–5376, 2020.

[23] C. Semini, V. Barasuol, J. Goldsmith, M. Frigerio, M. Focchi, Y. Gao, and D. G. Caldwell, "Design of the hydraulically actuated, torque-controlled quadruped robot hyq2max," *IEEE/ASME Transactions on Mechatronics*, vol. 22, no. 2, pp. 635–646, 2017.

[24] D. W. Haldane, J. K. Yim, and R. S. Fearing, "Repetitive extreme-acceleration (14-g) spatial jumping with salto-1p," in *2017 IEEE/RSJ International Conference on Intelligent Robots and Systems (IROS)*, 2017, pp. 3345–3351.

[25] G. Kenneally, A. De, and D. E. Koditschek, "Design principles for a family of direct-drive legged robots," *IEEE Robotics and Automation Letters*, vol. 1, no. 2, pp. 900–907, 2016.

[26] N. Kau, A. Schultz, N. Ferrante, and P. Slade, "Stanford doggo: An open-source, quasi-direct-drive quadruped," in *2019 International Conference on Robotics and Automation (ICRA)*, 2019, pp. 6309–6315.

[27] G. Bledt, P. M. Wensing, S. Ingersoll, and S. Kim, "Contact model fusion for event-based locomotion in unstructured terrains," in *2018 IEEE International Conference on Robotics and Automation (ICRA)*, 2018, pp. 4399–4406.

[28] S. Seok, A. Wang, M. Y. Chuah, D. Otten, J. Lang, and S. Kim, "Design principles for highly efficient quadrupeds and implementation on the mit cheetah robot," in *2013 IEEE International Conference on Robotics and Automation*, 2013, pp. 3307–3312.

[29] G. Kenneally and D. E. Koditschek, "Leg design for energy management in an electromechanical robot," in *2015 IEEE/RSJ International Conference on Intelligent Robots and Systems (IROS)*, 2015, pp. 5712–5718.

[30] Y. Chen and Q. Nguyen, "Adaptive force-based control for legged robots," *arXiv preprint arXiv:2011.06236*, 2020.

[31] J. Di Carlo, P. M. Wensing, B. Katz, G. Bledt, and S. Kim, "Dynamic locomotion in the mit cheetah 3 through convex model-predictive control," in *2018 IEEE/RSJ international conference on intelligent robots and systems (IROS)*. IEEE, 2018, pp. 1–9.

[32] C. Gehring, S. Coros, M. Hutter, M. Bloesch, M. A. Hoepflinger, and R. Siegwart, "Control of dynamic gaits for a quadrupedal robot," in *2013 IEEE International Conference on Robotics and Automation*, 2013, pp. 3287–3292.